17th World Conference on Earthquake Engineering, 17WCEE
Sendai, Japan - September 13th to 18th 2020

FAGILITY ANALYSIS OF HIGH-RISE RC FRAME CONSIDERING THE EFFECT OF MULTIPLE GROUND MOTION CHARACTERISTICS

C. XU[(1)], ZP. WEN[(2)]

[(1)] *Senior Engineer, Institute of Geophysics, China Earthquake Administration, xuchao@cea-igp.ac.cn*
[(2)] *Professor, Institute of Geophysics, China Earthquake Administration, wenzp@cea-igp.ac.cn*

Abstract

The damage potential of strong ground motion is commonly presented by an intensity measure (IM) in fragility evaluation of building structures. For high-rise buildings, scalar-valued intensity measures like peak ground acceleration usually hard to characterize the engineering properties and damage potential of ground motion. In this study, different alternative vector-valued IMs comprised of two ground motion parameters were used to present the ground motion potential to building structure. The sufficiency and efficiency of these IMs were compared for high-rise RC frame structures, and vector-valued IM based fragility surfaces were developed. For all the vector-valued IMs, spectral acceleration at fundamental period of the structure is considered as the first parameter. As the second parameter of the vectors, peak ground acceleration, peak ground velocity and spectral shape parameters were considered. Probabilistic seismic demand analysis of an eleven-story RC frame structure was conducted by means of incremental dynamic analysis, using maximum inter-story drift ratio as the engineering demand parameters. The efficiency and sufficiency of different vector-valued IMs was compared by means of regression and residual analysis. Then vector-valued IM based vulnerability surfaces revealing the relationship between the structural damage probability and two different ground motion parameters were developed. It is shown that the spectral shape and peak velocity also significantly affect the structural seismic response in addition to spectral acceleration at fundamental period of the structure. The residual of structural seismic demand can be significantly reduced by using vector-valued IMs comparing with scalar IMs, especially for high ground motion intensity levels. As a result of using more efficient vector-valued IMs in vulnerability analysis, the number of nonlinear dynamic analysis and the limitations of ground motion selection can be greatly reduced. Compared to scalar IM based vulnerability curves, vulnerability surfaces characterized by two ground motion parameters are more informative, which can reveal the impact of different ground motion parameters on structural response and damage probability.

Keywords: seismic fragility analysis; high-rise RC frame; vector-valued intensity measures; fragility surface

1. Introduction

The structural damage potential of ground motion is commonly characterized by a ground motion parameter called intensity measure (IM) in seismic vulnerability assessment. Seismic performance of buildings and strong ground motion data indicate that the structural seismic response and damage state depend on ground motion amplitude, spectrum, and duration characteristics simultaneously, and shown some obvious selective feature. For example, in 1962 Mexico 7.0 earthquake, high-rise buildings in Mexico City 200-300 km from the epicenter suffered serious damage with a recorded PGA of 0.05g; in 1966 US Parkfeld earthquake and 1972 US Stonecanyon earthquake, the damage was unusually slight with recorded PGA of 0.5g and 0.69g. Therefore, which IMs can well characterize the structural damage potential of ground motion is a key scientific issue for the study of vulnerability analysis as well as performance-based earthquake engineering.

The desirable features of an appropriate IM are efficiency and sufficiency [1]. The Efficiency means the ability to accurately predict the response of a structure subjected to earthquakes (i.e., comparatively small dispersion of structural response subjected to ground motions for a given IM). The sufficiency of IM is defined as one that renders structural responses subjected to ground motions for a given IM conditionally independent of other ground motion properties (i.e., no other ground motion information is needed to characterize the structural response). An efficient IM results in smaller variability of structural response, which implies fewer ground motion input for performance evaluation. A sufficient IM can reduce the complexity of record selection procedure based on seismic environment (i.e., magnitude, distance, site conditions, etc.).

Parameters such as seismic intensity and peak ground acceleration (PGA) are commonly used as IMs to quantify the structural performance in the past [2, 3, 4, 5]. There is an obvious disadvantage of logical cycle when using seismic intensity to predict structural damage. Although simple in concept and convenient for engineering application, peak ground acceleration shown some imperfections to relate the level of shaking to the expected damage, according to previous research and seismic performance [6, 7, 8]. More recently, the elastic spectral acceleration at first mode of vibration of the structure $Sa(T_1)$ has been thoroughly studied. The results shown that $Sa(T_1)$ can predict the structural response more efficient and sufficient than PGA [9, 10, 11]. Nevertheless, some limitations of $Sa(T_1)$ have been observed for high-rise buildings with significant higher-order modal response.

In summary, scalar-valued-IM-based vulnerability assessment can't reasonably account for the selective effect of structural damage and its mechanism caused by the uncertainty of ground motion. For this reason, different researchers suggested the use of vector-valued IMs and some progress has been made. (Baker et al., 2004, 2005; Kafali C, Grigoriu M, 2007; Rajeev P, Franchin P, Pinto PE, 2008; Sei'ichiro Fukushima, 2010; DM Seyedi et al., 2010). Baker has investigated vector-valued IMs consisting of spectral acceleration (SA) and some additional parameters related to the shape of response spectrum [12, 13]. Kafali and Grigoriu used a vector-valued IM expressed by two parameters: earthquake magnitude and source-to-site distance to characterize the damage probability of single degree-of-freedom systems [14]. Vector-valued IMs consisting of spectral value at two different periods has also been investigated for RC frames [15, 16]. Sei'ichiro Fukushima used PGA and PGV simultaneously as the IM to evaluate the performance of a seven-story-reinforced-concrete frame modeled as a lumped mass model with nonlinear springs [17]. They found that vector-valued IMs based on two parameters can predict the response of a structure with larger efficiency and sufficiency with respect to scalar-valued IMs (in principle, because more information about ground motion is included in the definition of its intensity)

Although previous researchers have shown that using more than one ground motion parameter can lead to a better prediction of the structural response and damage, very few have gone the extra step to develop a completely methodology for building vector-valued-IM-based vulnerability surface. The main goal of the present paper is to improve the presentation of ground motion by vulnerability surface for high-rise reinforced concrete frame structures through incremental dynamic analysis and to assess which vector-valued IM is more capable of predicting the damage probability of the structure with efficiency and

sufficiency. All the vector-valued IMs here considered are based on $Sa(T_1)$ as the first parameter because current hazard maps in many countries are mostly based on this parameter and several previous studies have discussed the advantages and disadvantages of using this parameter. As the second parameter of the vector, the peak ground velocity and spectral shape parameters are considered. Based on incremental dynamic analysis, the impacts of amplitude, spectrum and spectral shape of ground motion on structural response are investigated by means of regression and residual analysis. The sufficiency and efficiency of these alternative vector-valued IMs are studied. The vector valued vulnerability surfaces are then developed.

2. Structure model and ground motions

2.1 Structural model

A regular eleven-story RC frame structure designed according to the Chinese Seismic Design Code (GB50011-2010) was used for the case study. Geometrical characteristics of the structure are shown in Fig.1. Section dimensions of structural members and materials are list in Table 1.

A modified version of the DRAIN-2DX [18] program was used to establish the finite element model and perform the nonlinear dynamic response history analysis. The structural components were modeled by elastic-plastic beam-column element. A 2% strain-hardening ratio was considered to model the cyclic behavior of the structural components. P-Δ effect was considered by adding a geometric stiffness matrix to the stiffness matrix of each element. Different yield surfaces were specified to beam members and column members to distinguish the different mechanic behaviors. The fundamental period of vibration of the structure is 1.6s.

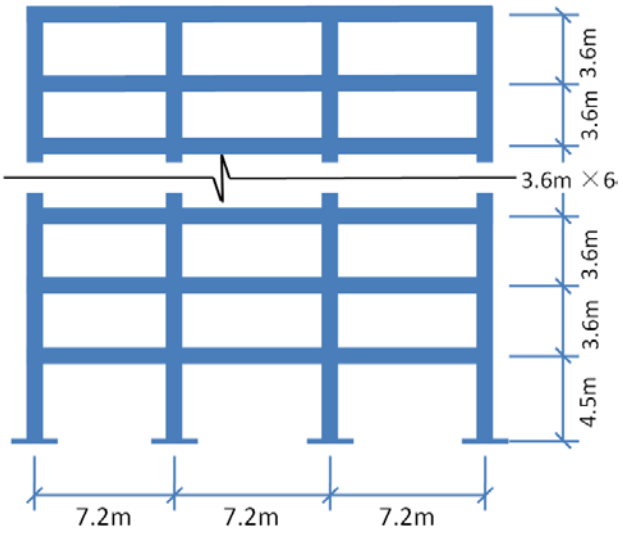

Fig.1 - The 11-story case-study RC frame

Table 1 - Section dimension and material of beams and columns

Srory number	Side column （mm×mm）	Center column （mm×mm）	Beam （mm×mm）	Concrete	Steel bar
1-6	600×600	650×700	300×700	C30	HRB335
7-11	550×550	600×650	300×700	C30	HRB335

2.2 Performance parameter and capacity of the structure

The maximum inter-story drift ratio (MIDR) is selected as the structural performance parameter, as it's the most common peak-response parameter in the seismic design codes to control the structural behavior. Five damage states are adopted, including undamaged, slight damage, moderate damage, intensive damage and collapse. Based on a large number of experiment data of RC frames, Gao Xiaowang proposed the method for calculating threshold MIDR for the onset of each damage state [19, 20]. Lognormal distribution was accepted to describe the threshold value. The capacity in terms of MIDR for the case study structure is calculated and shown in Table 2.

Table 2 – Structural capacity in terms of MIDR

Damage States	Slight Damage	Moderate Damage	Extensive Damage	Collapse
Mean Value	0.286%	0.654%	1.25%	3.6%
Coefficient of Variation	0.38	0.38	0.38	0.38

2.3 Ground motion records

The case study structures were subjected to forty ground motions to perform the vulnerability assessment. The records are taken from the PEER Strong Motion Database, their main characteristics are summarized in Table.3.

Table 3 - Characteristics of the Ground Motion Records

Record	Event	Year	Mw	Station	PGA(g)	PGV(cm/s)
1	Imperial Valley-06	1979	6.53	Calipatria Fire Station	0.078	13.3
2	Imperial Valley-06	1979	6.53	Chihuahua	0.27	12.42
3	Imperial Valley-06	1979	6.53	Compuertas	0.186	6.91
4	Imperial Valley-06	1979	6.53	El Centro Array #1	0.139	15.84
5	Imperial Valley-06	1979	6.53	El Centro Array #12	0.116	21.8
6	Imperial Valley-06	1979	6.53	El Centro Array #13	0.139	13.0
7	Imperial Valley-06	1979	6.53	Niland Fire Station	0.109	11.87
8	Imperial Valley-06	1979	6.53	Plaster City	0.111	17.79
9	Imperial Valley-06	1979	6.53	Parachute Test Site	0.057	5.39
10	Imperial Valley-06	1979	6.53	Westmorland Fire Sta	0.11	21.89
11	Loma Prieta	1989	6.93	Agnews State Hospital	0.172	25.94
12	Loma Prieta	1989	6.93	Capitola	0.443	29.21
13	Loma Prieta	1989	6.93	Coyote Lake Dam (Downst)	0.16	13.04
14	Loma Prieta	1989	6.93	Gilroy Array #3	0.367	44.66
15	Loma Prieta	1989	6.93	Gilroy Array #4	0.212	37.86
16	Loma Prieta	1989	6.93	Gilroy Array #7	0.225	16.4
17	Loma Prieta	1989	6.93	Halls Valley	0.134	15.4
18	Loma Prieta	1989	6.93	Hollister Diff. Array	0.279	35.57
19	Loma Prieta	1989	6.93	Palo Alto - SLAC Lab	0.194	37.45
20	Loma Prieta	1989	6.93	Salinas - John & Work	0.112	15.68
21	Loma Prieta	1989	6.93	Sunnyvale - Colton Ave.	0.207	37.28
22	Northridge-01	1994	6.69	Arcadia - Arcadia Av	0.104	7.32
23	Northridge-02	1994	6.69	Baldwin Park - N Holly	0.123	8.17

24	Northridge-03	1994	6.69	Canoga Park - Topanga Can	0.42	60.69
25	Northridge-04	1994	6.69	Downey - Birchdale	0.171	8.12
26	Northridge-05	1994	6.69	Elizabeth Lake	0.109	8.96
27	Northridge-06	1994	6.69	Glendale - Las Palmas	0.206	7.39
28	Northridge-07	1994	6.69	LA - Centinela St	0.322	22.86
29	Northridge-08	1994	6.69	LA - Fletcher Dr	0.24	26.22
30	Northridge-09	1994	6.69	LA - N Faring Rd	0.273	15.8
31	Northridge-10	1994	6.69	LA - Pico & Sentous	0.186	14.23
32	Northridge-11	1994	6.69	LA - Saturn St	0.474	34.48
33	Northridge-12	1994	6.69	LA - Univ. Hospital	0.214	10.76
34	Northridge-13	1994	6.69	La Crescenta - New York	0.159	11.28
35	Northridge-14	1994	6.69	Lawndale - Osage Ave	0.153	7.95
36	San Fernando	1971	6.61	LA - Hollywood Stor FF	0.174	14.85
37	Superstitn Hills	1987	6.54	Brawley Airport	0.156	13.89
38	Superstitn Hills	1987	6.54	Calipatria Fire Station	0.247	14.54
39	Superstitn Hills	1987	6.54	Plaster City	0.186	20.62
40	Superstitn Hills	1987	6.54	Poe Road (temp)	0.446	35.71

3. Methodology

3.1 Vector-valued ground motion Ims

Four different vector-valued ground motion IMs are considered to evaluate the seismic vulnerability of the structure. All the vector-valued IMs are based on spectral acceleration at fundamental period of the structure $S_a(T_1)$ as the first parameter (denote as IM_1) because current hazard maps in many countries are mostly based on this parameter and several previous studies have discussed the advantages and disadvantages of using this parameter. The second parameters (denote as IM_2) are defined as:

$$R_{PGV,S_a} = PGV / S_a(T_1) \tag{1}$$

$$R_{T_1,T_2} = S_a(T_2) / S_a(T_1) \tag{2}$$

$$Np = S_{a,avg}(T_M,...T_N) / S_a(T_1) \tag{3}$$

$$S_{a,avg}(T_M,...T_N) = (\prod_{i=M}^{N} S_a(T_i))^{1/(N-M+1)} \tag{4}$$

$$\varepsilon(T_1) = \ln S_a(T_1)_{record} - \mu_{\ln S_a(T_1)} / \sigma_{\ln S_a(T_1)} \tag{5}$$

It is recalled that the normalization of IM_2 with respect to the spectral acceleration at the fundamental period, lets IM_2 be independent with respect to the scaling level. In Eq.(1), the peak ground velocity (PGV) is selected to investigate the impact of peak ground motion on structural response. The parameter R_{T_1,T_2} in Eq.(2) is the ratio of the spectral acceleration at period T_2 divided by spectral acceleration at period T_1. The parameter Np in Eq.(3) is the value of $S_{a,avg}(T_M,...T_N)$ divided by spectral acceleration at period T_1, where $S_{a,avg}(T_M,...T_N)$ in In Eq.(4) is the geometric mean of spectral acceleration between a specific period range T_M to T_N. Parameter $\varepsilon(T_1)$ in In Eq.(5) is defined as a measure of the difference between the spectral acceleration of a record and the mean of a ground motion prediction equation at the given period T_1. R_{T_1,T_2}, Np and $\varepsilon(T_1)$ include information about the spectral shape, which may be expected to account for the effect of higher mode response and structural softening.

3.2 Method for developing vulnerability surface

Vulnerability characterized by vector-valued IMs is developed via incremental dynamic analysis (IDA) [21]. Here, IDA is first performed by varying IM_1 (in this case $S_a(T_1)$) until the EDP value (MIDR) of interest is obtained. Then the impact of the second parameter IM_2 on structural response is accounted as follow.

IDA curves are plotted along with IM_2, as shown in Fig.2(a). The points where each IDA curve first reaches the EDP level of interest (MIDR=0.01 for this example) define a set of IM capacity values, indicated by red circles in Fig.2(a). These IM capacity points are plotted in Fig.2(b). It is apparent in Fig.2(b) that in this example IM_2 can explain part of the variation of IM_1 capacity (i.e. the $IM_{1,cap}$ values tend to be larger for smaller values of IM_2, which means that the structural response tends to be larger for larger IM_2 when records are scaled to a specific IM_2 level). In Fig.2(b), the conditional distribution of $\ln IM_{1Cap}$ appears to be linearly dependent upon IM_2, so linear regression can be used to find the conditional mean of $\ln IM_{1,cap}$ given IM_2 for a specific EDP level:

$$\ln IM_{1,cap} / EDP, IM_2 = \beta_0 + \beta_1 \ln IM_2 + \ln \varepsilon \tag{6}$$

Where β_0 and β_1 are constant coefficients estimated from linear regression using the data points from Fig. 2(b). The standard deviation of the regression residuals, $\sigma_{\ln \varepsilon}$, is estimated from the observed prediction errors. The conditional distribution of $\ln IM_{1,cap}$ is assumed to be Gaussian, then the vulnerability can be computed as:

$$F_{DS/IM_1,IM_2}(IM_1 = x_1, IM_2 = x_2) = \Phi\left(\frac{\ln x_1 - \mu_{\ln IM_{1,cap}/EDP=\exp(\mu_{\ln EDP_C/DS}),IM_2=x_2}}{\sqrt{\beta^2_{IM_{1,cap}/EDP=\exp(\mu_{\ln EDP_C/DS}),IM_2=x_2} + \beta^2_{EDP_C/DS}}}\right) \tag{7}$$

where $F_{DS/IM_1,IM_2}(IM_1 = x_1, IM_2 = x_2)$ is the exceeding probability of a given damage state (DS), given $IM_1 = x_1$, $IM_2 = x_2$; Φ is the cumulative distribution function (CDF) of the standard Gaussian distribution; $\mu_{\ln EDP_C/DS}$ and $\beta_{EDP_C/DS}$ are the mean value and standard deviation of the capacity in terms of the lnEDP for a given damage state. $\mu_{\ln IM_{1,cap}/EDP=\exp(\mu_{\ln EDP_C/DS}),IM_2=x_2}$ and $\beta_{IM_{1,cap}/EDP=\exp(\mu_{\ln EDP_C/DS}),IM_2=x_2}$ are the mean value and standard deviation of $\ln IM_{1,cap}$ given $IM_2 = x_2$ for a specific EDP level $EDP = \exp(\mu_{\ln EDP_{CAP}/DS})$, which can be estimated by Eq.(7).

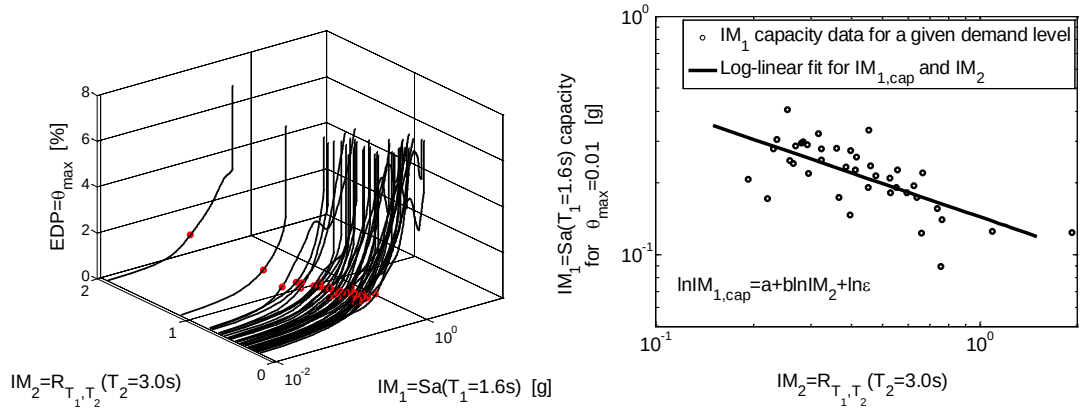

(a) (b)

Fig.2 - Estimation of structural response by means of vector-valued IM via IDA: (a) IDA curves plotted with a vector-valued IM and IM capacity points for a given EDP level; (b) IM_1-IM_2 pairs corresponding to occurrence of the given EDP, see red circles in Fig.2(a), and the log-linear regression

4. Results of vulnerability analysis

4.1 Comparison of different vector-valued IMs

As show in Fig.2(a), IDA curves based on a vector valued intensity measure $S_a(T_1)$ and $R_{T_1,T_2}(T_2 = 3.0s)$ are plotted. The points where IDA curve first reaches maximum inter-story drift ratio $\theta_{\max}$ of 1% (indicated by red circles) define a set of IM capacity values. These points are plotted in Fig.2(b). It is apparent in Fig.2(b) that the $S_a(T_1)$ capacity (denoted by $S_a(T_1)_{cap}$) tends to be larger for smaller $R_{T_1,T_2}(T_2 = 3.0s)$, in other words, the structural response tends to be larger for larger $R_{T_1,T_2}(T_2 = 3.0s)$ when records are scaled to a specific $S_a(T_1)$ level, which means that $R_{T_1,T_2}(T_2 = 3.0s)$ can explain part of the variation of $S_a(T_1)$ capacity or variation of structural response. In Fig.2(b) the conditional distribution of $\ln S_a(T_1)_{cap}$ appears to be linearly dependent upon $\ln R_{T_1,T_2}(T_2 = 3.0s)$, so log-linear regression can be used to find the conditional mean and standard deviation of $\ln S_a(T_1)_{cap}$ given $R_{T_1,T_2}(T_2 = 3.0s)$, i.e.: $\mu_{\ln S_a(T_1)_{cap}}$ and $\beta_{S_a(T_1)_{cap}}$. Then T_2 is selected over arrange of possible values for R_{T_1,T_2} to maximum efficiency, or minimize $\beta_{S_a(T_1)_{cap}}$. A plot of fractional reduction in $\beta_{S_a(T_1)_{cap}}$ (compared to scalar valued IM $S_a(T_1)$) by R_{T_1,T_2} for different T_2 values is shown in Fig.3, where the inter-story drift ratio demand is 1%. We see that the optimal T_2 value is 2.4s, which can result in a minimum dispersion of $\beta_{S_a(T_1)_{cap}}$.

This optimal T_2 value is only relevant for a single level of drift demand. We can repeat the same calculation for different levels of drift demand and the result is shown in Fig.4. It is apparent that the optimal T_2 value varies depending on the drift demand level. For lower drift demand level, for example $\theta_{\max} = 0.001$, we find that the optimal T_2 is about 0.5s. This is near 0.54s, the second-mode period of vibration of the structure. For higher level of drift demand, for example $\theta_{\max} \geq 0.01$, we find that the optimal T_2 is larger than T_1, here T_2=2.4s is the best choice.

If one were to combine engineering intuition with the results of Fig.3 and Fig.4, the following conclusion might be drawn, keeping in mind that the seismic response of this eleven-story structure is first-mode dominated (mass-participation coefficient of first-mode is 0.83): for lower level of drift demand with no structural nonlinearly, the optimal T_2 to incorporate would be near the second-mode period of vibration of the structure. Note that at this level of drift demand the structure stays linear, an optimal T_2 for R_{T_1,T_2} which can account for higher mode effect would be more efficient. And for higher level of drift demand such as $\theta_{\max} \geq 0.01$, then the optimal T_2 will be larger than T_1. Note that for this drift demand level significant nonlinear behavior appears in the structure, and the fundamental period of the structure would be lengthened because of structural softening effect, so R_{T_1,T_2} with T_2 values lager than T_1 would be more efficient. For this eleven-story structure, T_2=1.5T_1 is the best choice. It is also apparent that the fractional reduction in dispersion of $S_a(T_1)_{cap}$ by using R_{T_1,T_2} for larger T_2 values at high level of drift demand is much more significant than by using R_{T_1,T_2} for smaller T_2 values at low level of drift demand, which means that the impact of structural softening caused by nonlinearly on response is much more significant than higher mode effect.

Using the same method, fractional reductions in dispersion of $S_a(T_1)_{cap}$ by means of Np, R_{PGV,S_a} and $\varepsilon(T_1)$ are calculated. The efficiency of different IMs is compared, as shown in Fig.5. Here Np is calculated with the period between 1.6s and 3.2s. We find that Np is the most efficient parameter for a vector IM to evaluate the structural response, which indicates that spectra shape in a range of period larger than T_1 is an important character of records for structural seismic demand analysis.

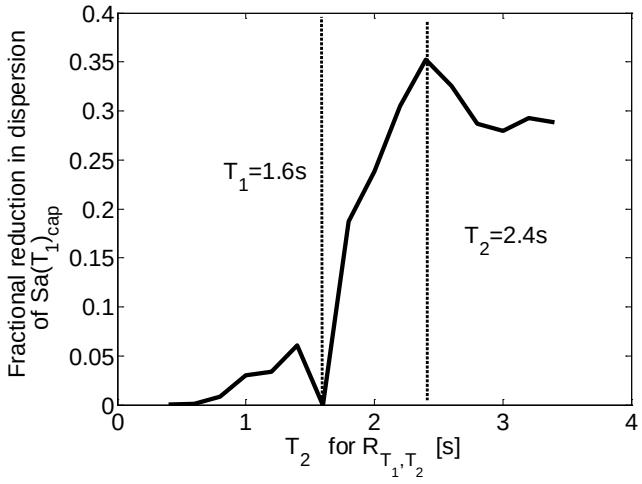

Fig.3 - Fractional reduction in dispersion of $S_a(T_1)_{cap}$ by R_{T_1,T_2} for T_2 between 0.3s and 3.4s for a demand level θ_{max} =1%

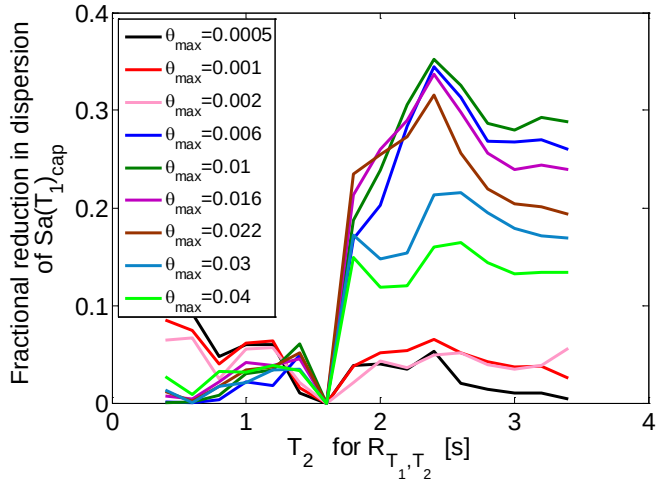

Fig.4 - Fractional reduction in dispersion of $S_a(T_1)_{cap}$ by R_{T_1,T_2} for T_2 between 0.3s and 3.4s for different demand levels

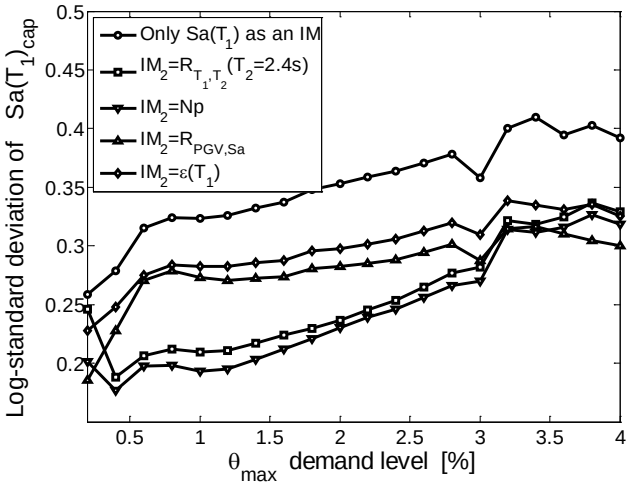

Fig.5 - Dispersion of $S_a(T_1)_{cap}$ at different demand levels by means of different vector-valued IMs

4.2 Vector-valued fragility surfaces

Fig.6 shows the developed collapse fragility surfaces based on a vector-valued IMs. These surfaces can be visualized as fragility curves by projecting the surface onto the $S_a(T_1)$ planes, as shown in Fig.7. These figures demonstrate the wide variation between fragility curves based on scalar-valued intensity measure, e.g. $S_a(T_1)$. Scalar-valued IM such as $S_a(T_1)$ based fragility curves can't incorporate the variability in ground motion as measured by other parameters. It can be seen in Fig.7 that there can be a discrepancy of up to 70% between two curves (i.e., collapse probability of 10% for Np =0.3 and 80% for Np =0.9 at $S_a(T_1)$=0.5g). Compared to scalar IM based fragility curves, fragility surfaces characterized by two ground motion parameters are more informative, which can reveal the impact of different ground motion parameters on structural response and damage probability.

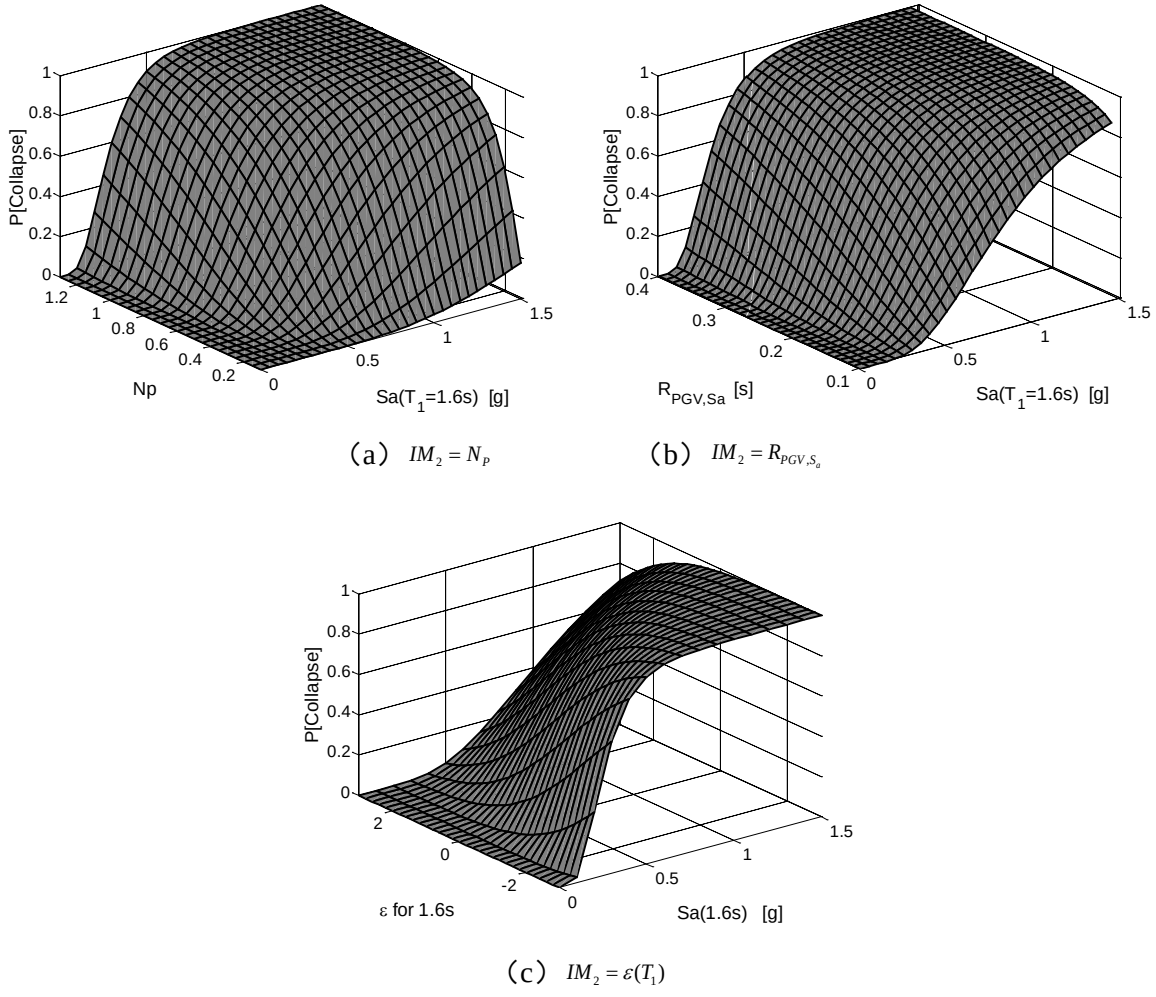

(a) $IM_2 = N_P$ (b) $IM_2 = R_{PGV,S_a}$

(c) $IM_2 = \varepsilon(T_1)$

Fig.6 - Collapse fragility surfaces based vector valued IMs: (a) $IM_2 = N_P$, (b) $IM_2 = R_{PGV,S_a}$, (c) $IM_2 = \varepsilon(T_1)$

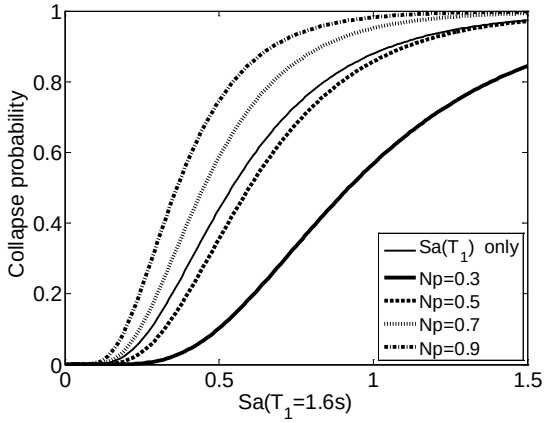

(a) $IM_2 = N_P$

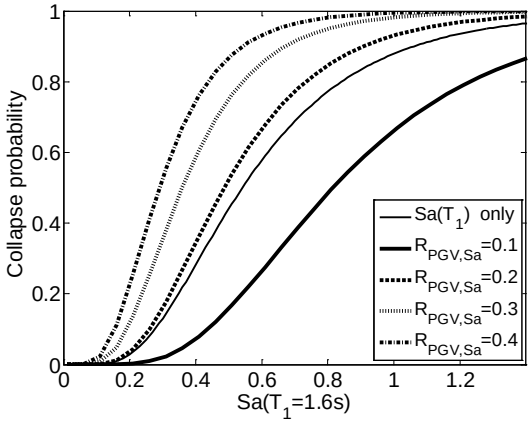

(b) $IM_2 = R_{PGV,S_a}$

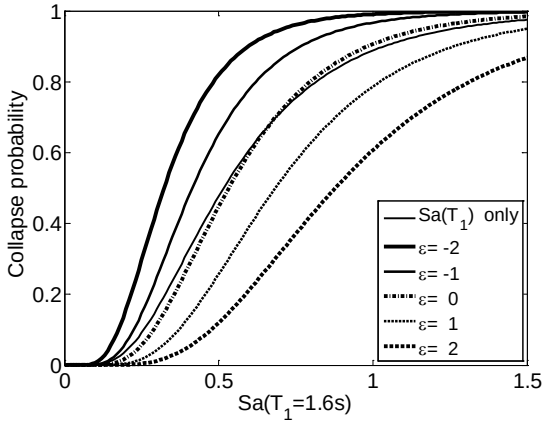

(c) $IM_2 = \varepsilon(T_1)$

Fig.7 - $S_a(T_1)$ based fragility curves at different IM_2 values

5. Conclusion

Alternative vector-valued IMs consisting of two parameters of ground motions were used to quantify the damage potential of ground motions. The sufficiency and efficiency of the IMs were studied for high-rise RC frame structures and vector-valued IM based fragility surfaces were developed. It is found that vector-valued IMs consisting of two parameters are more sufficient and efficient than scalar-valued IM $S_a(T_1)$. When R_{T_1,T_2} is selected as the second parameter of the vector-valued IM, its sufficiency varies depending on the nonlinearity of the structure and the choice of T_2. At low level of drift demand the structure remains in linear stage, an optimal T_2 near the second mode period of the structure for R_{T_1,T_2} which can account for higher mode effect would be more efficient. For high level of drift demand, significant nonlinear behavior appears in the structure, and the fundamental period of the structure would be lengthened because of structural softening effect, so R_{T_1,T_2} with T_2 values lager than T_1 would be more efficient. For this eleven-story structure, T_2=1.5T_1 is the best choice. Np calculated with the period between 1.6s and 3.2s is the most efficient parameter for a vector IM to evaluate the structural response, which indicates that spectra shape in a range of period larger than T_1 is an important character of records for structural seismic demand analysis. Fragility surfaces based on vector-valued IMs are developed. Fragility surfaces characterized by two ground motion parameters are more informative, which can reveal the impact of different ground motion parameters on structural response and damage probability.

6 Acknowledgements

This work is financially supported by National Key R&D Program of China (2018YFC1504602-04). The contributions of anonymous reviewers and editors are also acknowledged.

7. References

[1] Luco N (2002): Probabilistic seismic demand analysis, SMRF connection fractures, and near-source effects. *PhD Thesis*, Stanford University.

[2] Hwang HHM, Low YK (1989): Seismic reliability analysis of plane frame structures. *Probabilistic Engineering Mechanics*, **4**(2): 74-84.

[3] Hwang HHM, Jaw JW (1990): Probabilistic damage analysis of structures. *ASCE Journal of Structural Engineering*, **116**(7): 1992-2007.

[4] Singhal A, Kiremidjian AS (1996): Method for probabilistic evaluation of seismic structural damage. *ASCE Journal of Structural Engineering*, **122**(12): 1459-1467.

[5] Singhal A, Kiremidjian AS (1998): Bayesian updating of fragilities with application to RC frames. *ASCE Journal of Structural Engineering*, **124**(8): 922-929.

[6] Elenas A (2000): Correlation between seismic acceleration parameters and overall structural damage indices of buildings. *Soil Dynamics and Earthquake Engineering*, **20**: 93-100.

[7] Gardoni P, Mosalam KM, Der Kiureghian A (2003): Probabilistic seismic demand models and fragility estimates for RC bridges. *Journal of Earthquake Engineering*, **7** (Special Issue 1):79-106.

[8] Schotanus MIJ, Franchin P, Lupoi A, Pinto PE (2004): Seismic fragility analysis of 3D structures. *Structural Safety*, **26** (4):421-441.

[9] Ellingwood BR, Celik OC and Kinali K (2007): Fragility assessment of building structural systems in Mid-America. *Earthquake Engineering and Structural Dynamics*, **36**(3):1935-1952.

[10] Ellingwood BR (2001): Earthquake risk assessment of building structures. *Reliability Engineering and System Safety*, **74**: 251-262.

[11] Kafali C, Grigoriu M (2004): Seismic fragility analysis. *Proceedings of the Ninth ASCE Specialty Conference on Probabilistic Mechanics and Structural Reliability (PMC2004)*. Albuquerque, NM.

[12] Baker JW, Cornell CA (2004): Choice of a vector of ground motion intensity measures for seismic demand hazard analysis. *Proceedings of the Thirteenth World Conference on Earthquake Engineering*, Vancouver, Canada.

[13] Baker JW, Cornell CA (2005): A vector-valued ground motion intensity measure consisting of spectral acceleration and epsilon. *Earthquake Engineering and Structural Dynamics*, **34**: 1193-1217.

[14] Kafali C, Grigoriu M (2007): Seismic fragility analysis: application to simple linear and nonlinear systems. *Earthquake Engineering and Structural Dynamics*, **36**:1885-1900.

[15] Rajeev P, Franchin P, Pinto PE (2008): Increased accuracy of vector-IM-based seismic risk assessment. *Journal of Earthquake Engineering*, **12**:111-124.

[16] Seyedi DM, Gehl P, Douglas J (2010): Development of seismic fragility surfaces for reinforced concrete buildings by means of nonlinear time-history analysis. *Earthquake Engineering and Structural Dynamics*, **39**: 91-108.

[17] Sei'ichiro Fukushima (2010): Vector-valued fragility analysis using PGA and PGV simultaneously as ground-motion intensity measures. *Journal of Disaster Research*, , **5**(4):407-417

[18] Prakash V, Powell G, Campbell S (1993): DRAIN-2DX: basic program description and user guide. *Report No. UBC/SEMM-93/17*, University California at Berkeley, Berkeley, CA.

[19] Gao XW, Shen JM (1994): A simplified method for calculating limit story drift of reinforced concrete frame. *Journal of Building Structures*, **14**(2): 28-37.

[20] Gao XW, Shen JM (1993): Aseismic reliability analysis of various damage states in reinforced concrete frame structure. *Building Science*, **26** (1): 3-11.

[21] Vamvatsikos D, Cornell CA (2002): Incremental dynamic analysis. *Earthquake Engineering & Structural Dynamics*, **31** (3), 491-514.

